JOM, Vol. 70, No. 5, 2018
https://doi.org/10.1007/s11837-018-2779-2

On the Importance of Adiabatic Heating on Deformation Behavior of Medium-Manganese Sheet Steels

RADHAKANTA RANA,[1,2,3] EMMANUEL DE MOOR,[1,4] JOHN G. SPEER,[1,5] and DAVID K. MATLOCK[1,6]

1.—Advanced Steel Processing and Products Research Center (ASPPRC), Colorado School of Mines, Golden, CO 80401, USA. 2.—*Present address:* Tata Steel, Wenckebachstraat 1, 1970 CA IJmuiden, The Netherlands. 3.—e-mail: rana9433@gmail.com. 4.—e-mail: edemoor@mines.edu. 5.—e-mail: jspeer@mines.edu. 6.—e-mail: dmatlock@mines.edu

The effects of adiabatic heating during deformation of a medium-manganese transformation-induced plasticity steel containing 10.1Mn-1.68Al-0.14C-0.2Si (wt.%) processed with initially 57 vol.% retained austenite were investigated over the temperature range from − 60°C to 100°C at strain rates from 0.002 s^{-1} to 0.2 s^{-1}. Tensile tests were performed on specimens immersed in isothermal baths, which reduced but did not completely eliminate adiabatic heating. The specimen temperature depended on the extent of adiabatic heating, which increased with strain and strain rate. The measured properties primarily reflected the effects of temperature on austenite stability and the corresponding resistance of austenite transformation to martensite with strain. Changes in austenite stability were monitored by measurements of austenite fractions at a specific strain and observation of microstructures after deformation. The results of this study provide a basis to identify input material parameters required for numerical models applicable to sheet metal forming of medium-Mn steels.

INTRODUCTION

Medium-manganese sheet steels with Mn contents typically between 5 wt.% and 12 wt.%, processed to have microstructures containing retained austenite contents up to approximately 60 vol.% distributed in high-strength fine-grained ferritic matrices, have received considerable attention recently as candidates for achieving strength–ductility combinations characteristic of third-generation advanced high-strength steels (3GAHSS) for use in automobile manufacture.[1–8] The presence of retained austenite with controlled stability [i.e., enhanced resistance to deformation-induced transformation to martensite, the classic transformation-induced plasticity (TRIP) effect] is critical to form high-strength steels with high ductilities required to ensure excellent formability.[9–11] Among other factors, austenite stability increases with Mn content (in this case controlled by partitioning during intercritical annealing) and with an increase in deformation temperature. Detailed mechanistic analyses of the effects of alloying and temperature on the strain-induced transformation of austenite to martensite, and the importance of stacking fault energy, are considered elsewhere.[12–14]

Currently, in automotive and related industries, considerable efforts are focused on development of numerical models to guide product design and forming operations.[15–17] The primary input to most forming models is the stress–strain behavior of the material of interest, obtained using standard test techniques at room temperature in air, often over a range of strain rates. For automotive forming operations, traditional steels in current use contain limited amounts of retained austenite, and room-temperature data are typically sufficient for models which describe cold stamping operations. For these materials (e.g., high-strength low-alloy steels, dual-phase steels, and others with primarily ferritic microstructures), the microstructure and property changes during forming are primarily a function of strain and, to a much lesser extent, temperature. However, for many new 3GAHSS products which contain significant amounts of retained austenite, incorporation of a complete understanding of the

(Published online February 27, 2018)

effects of temperature on steel properties will be critical for development of accurate model predictions.[9,10]

In commercial sheet steel forming operations, the deformation temperature at any point in the operation reflects a combination of the starting temperature and local temperature increases due to friction with tools and adiabatic heating of the sheet due to deformation. Recently, Pereira and Rolfe[18] presented a finite element analysis to describe friction- and deformation-induced heating during sheet metal forming and validated the predictions of their model with measurements on a novel semi-industrial stamping test facility. Their results, based on a single stamping operation, showed that, for two high-strength low-alloy steels (HSLA300 and HSLA400) and two dual-phase steels (DP590 and DP780) with tensile strength between 485 MPa and 880 MPa, the effects of friction and adiabatic heating can lead to die temperatures in excess of 180°C and blank temperatures of 110°C for tests with punch speed at the beginning of the forming operation of 300 mm/s. Due to high contact forces, higher-strength steels are expected to exhibit even greater temperature increases. Furthermore, steady-state die temperatures in production operations will significantly exceed the temperatures observed in single stamping events. The importance of adiabatic heating observed in forming also extends to crash situations, where predictions of vehicle energy absorbance will also depend on the temperature-dependent deformation behavior of the materials.

To incorporate the deformation behavior of medium-manganese steels into numerical models, complete understanding of the effects of deformation conditions, i.e., temperature, strain rate, and stress state, on the transformation behavior of retained austenite to martensite and the corresponding effects of martensite on strength and ductility is required. The current study was designed to assess, for a single medium-Mn steel, the extent to which adiabatic heating during tensile testing alters the stress–strain behavior. The results provide insight into potential modifications to material constitutive relationships which will be required for data incorporated into quantitative predictive models of sheet metal forming of new AHSS products with high retained austenite content.

EXPERIMENTAL PROCEDURES

A laboratory-produced ingot of Fe-10.1Mn-1.68Al-0.14C-0.2Si (wt.%) alloy (denoted as 10MnAl steel) was processed to 1.5-mm-thick sheets by hot and cold rolling with a final cold reduction of 62%. The cold-rolled sheets were intercritically annealed for 16 h at 640°C to produce a final microstructure consisting of 57 vol.% retained austenite, 31 vol.% fine-grained (nominally 1–2 μm) ferrite, and 12 vol.% martensite.[3] While the amount of retained austenite was estimated from x-ray diffraction (XRD) measurements, the ferrite fraction was calculated by Thermo-Calc and the remainder of the microstructure was assumed to be martensite.[2]

ASTM E-8 subsized tensile samples with thickness equal to the as—rolled sheet were machined with the tensile axis perpendicular to the rolling direction and a nominally 33-mm-long reduced gage section with width of 6.4 mm. Single-sample tensile tests were conducted in air at room temperature and with samples immersed in isothermal baths at temperatures between − 60°C and 100°C (cooled in ethanol for $T \leq 20$°C or heated in oil). Tensile tests were performed at engineering strain rates of 0.002 s^{-1}, 0.02 s^{-1}, and 0.2 s^{-1}, and strain was measured over a 25.4-mm gage length using a submersible extensometer capable of strain measurements to failure. Sample temperatures were obtained with type K thermocouples spot-welded to the gage length surface. XRD measurements on samples deformed to a strain of 20% (which is in the uniform deformation regime) as well as to fracture were used to determine retained austenite contents. Undeformed and deformed microstructures were observed on polished and etched (2 vol.% nital) metallographic samples by high-resolution scanning electron microscopy (SEM) from longitudinal sections which contained the rolling and normal directions after etching.

RESULTS AND DISCUSSION

Tensile Properties, Austenite Stability, and Microstructure

Complete stress–strain curves in isothermal baths were obtained over the range of temperatures and strain rates of interest. Figure 1a presents a selected set of results for samples tested at an engineering strain rate of 0.002 s^{-1}. These results illustrate the strong effect of test temperature on the deformation behavior over a narrow temperature range above and below room temperature. The effects of temperature shown in Fig. 1a are characteristic of the behavior at strain rates of 0.02 s^{-1} and 0.2 s^{-1}. At all test temperatures, yielding was associated with a sharp yield point and a region of discontinuous yielding characterized by yield point elongation (YPE). The shapes of the plastic deformation regimes of the tensile curves systematically changed with an increase in temperature. At low temperatures, immediately after YPE, the curves were essentially parabolic with a high rate of work hardening and the presence of a short sigmoidal region (i.e., a region where the slope of the stress–strain curve initially increased with strain to a maximum value and then decreased to form the characteristic parabolic shape where the slope continually decreased with increase in strain). With an increase in temperature, the average work-hardening rates decreased, the strength decreased, and the strain range associated with the sigmoidal behavior

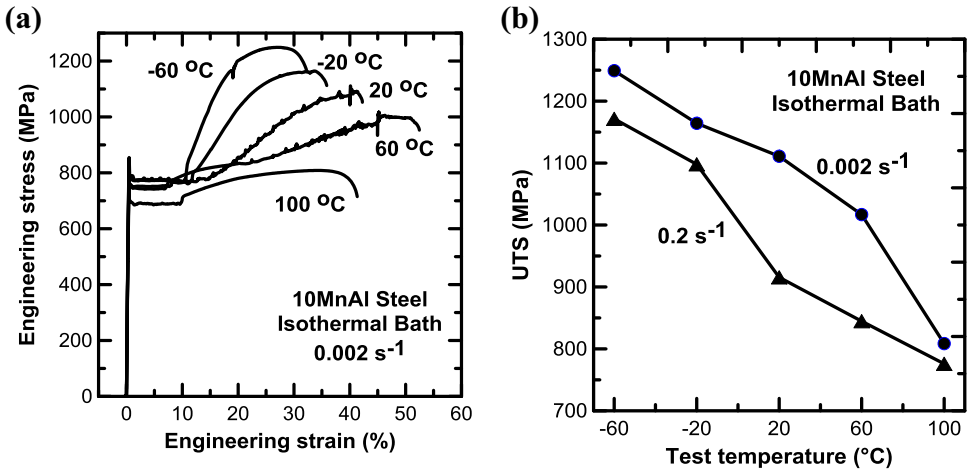

Fig. 1. Effect of temperature on tensile properties of 10MnAl steel immersed in isothermal baths. (a) Engineering stress versus engineering strain at an imposed engineering strain rate of 0.002 s^{-1}. (b) Comparison of effect of temperature on UTS values obtained at a strain rate of 0.002 s^{-1} and 0.2 s^{-1}. Adapted from Ref. 3.

increased, up to test temperature of 60°C. At the highest test temperature of 100°C, the sigmoidal region was essentially absent. Also apparent from the tests at 20°C and 60°C were serrations (i.e., rapid, incremental load decreases) associated with continuous incremental nucleation and propagation of deformation bands within the strain-hardening regime, a feature characteristic of medium-Mn steels.[19] Figure 1b shows the effect of test temperature on the ultimate tensile strength (UTS) of samples tested at 0.2 s^{-1} and 0.002 s^{-1}. At both strain rates, a significant decrease in strength was observed over the temperature range of interest. Furthermore, Fig. 1b reveals that, for any particular test temperature, lower UTS values were observed at the higher strain rate, indicating negative strain rate sensitivity of stress, an observation also recently reported in a study on twinning-induced plasticity (TWIP) steels.[20]

The deformation behavior illustrated in Fig. 1 for the high-austenite-containing medium-Mn steel is similar to that of stainless steels containing metastable austenite reported in literature.[21,22] Specifically, the transition in deformation behavior shown in Fig. 1a and the inverse strain rate sensitivity in Fig. 1b have been shown[23] to depend directly on the effect of temperature on austenite stability (i.e., resistance to deformation-induced transformation to martensite with strain). At low temperatures, austenite is unstable and rapidly transforms with strain, resulting in a rapid increase in strength due to significant martensite formation at low strains. With an increase in test temperature, austenite stability increases and transformation to martensite is delayed to higher strains, producing the sigmoidal stress–strain curve shape and stabilizing deformation leading to the high ductilities observed at intermediate test temperatures. With an increase in strain rate, due to adiabatic heating, the temperature of the specimen also increases more at the higher strain rate, leading to an increase in austenite stability and a decrease in the amount of strengthening obtained from the presence of deformation-induced martensite, resulting in negative strain rate sensitivity.

The transformation behavior of retained austenite to martensite as a function of test temperature for the two strain rates considered in Fig. 1b is presented in Fig. 2. Measurements of austenite volume fractions on the as—processed samples prior to deformation, after a strain of 20% in interrupted tensile tests, and in deformed uniform gage sections of failed samples were used to assess the effects of testing variables on austenite stability. Figure 2a shows calculated "austenite transformation ratios," defined as the ratio of the amount of austenite transformed at a strain of 20% to the amount initially present versus test temperature for data obtained at the two strain rates in Fig. 1b. A transformation ratio of 0 indicates no transformation of retained austenite, while a value of 1 indicates that all of the austenite initially present transformed to martensite at the imposed strain, thus this parameter quantifies the austenite stability with strain. For both strain rates, the austenite transformation ratio decreased with an increase in test temperature, confirming the effect of temperature on austenite stability. In addition, the transformation ratio was higher at all test temperatures for the lower strain rate, an observation that confirms that austenite was more stable in the sample deformed at the higher rate. The results below will show that the increased stability with strain rate is a direct consequence of adiabatic heating, even in the isothermal baths.

Figure 2b shows the changes in austenite content with engineering strain for samples deformed at all test temperatures at an engineering strain rate of 0.2 s^{-1}. Similar datasets were obtained at the other two strain rates. At – 60°C, the majority of the

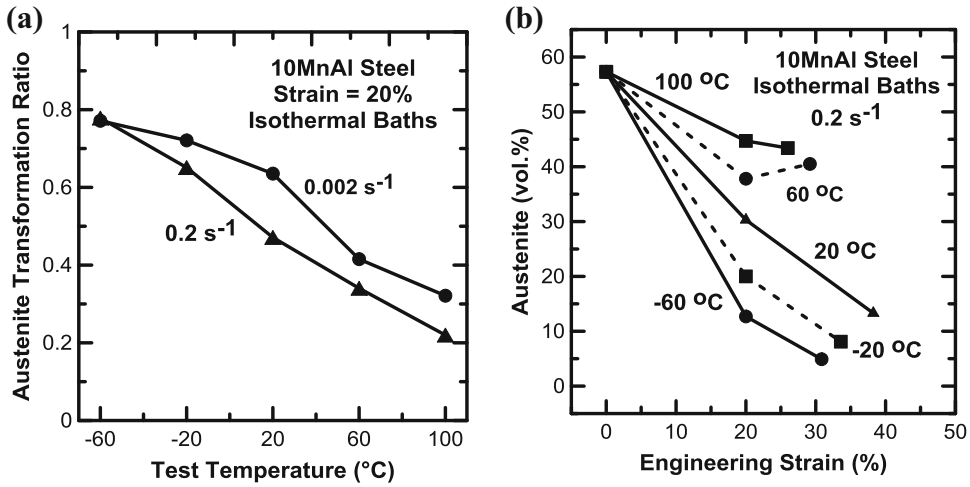

Fig. 2. (a) Comparison of effects of strain rate on austenite transformation ratio as function of test temperature measured on samples tested in isothermal baths to 20% strain. (b) The effects of strain on transformation of retained austenite as function of temperature (data shown up to uniform strain at instability).

initial austenite transformed at strains less than 20%, resulting in the high work-hardening rate shown in Fig. 1a. With an increase in temperature, Fig. 2b shows that the strain dependence decreased, which also correlates with the observations in Fig. 1b that the work-hardening rate decreased with an increase in test temperature due to decreasing amounts of deformation-induced martensite contributing to strength.

Figure 3 shows the microstructure of the as-annealed material (Fig. 3a) and after deformation at a strain rate of 0.2 s^{-1} to a strain of 20% at – 60°C (Fig. 3b) and 100°C (Fig. 3c), the two temperature extremes in this study. As summarized elsewhere,[3] in the annealed condition (Fig. 3a), the ultrafine (1–2 μm grain size) microstructure consisted of ferrite (F), austenite (A), and martensite or martensite–austenite constituents (MA) (evidenced by regions of high surface relief). After deformation, etched martensite was evident in previously austenitic areas, particularly in the sample deformed at – 60°C (Fig. 3b). These microstructural observations correlate with the austenite stability quantified in Fig. 2. At the lower test temperature of – 60°C, the stability of austenite was lower and therefore more austenite transformed to martensite than at 100°C.

Effects of Adiabatic Heating on Deformation Behavior

The test temperatures referenced in the discussion above are the stabilized bath temperatures at which the tensile tests were conducted. However, the actual specimen temperatures increased with strain due to adiabatic heating of the specimens even though the specimens were immersed in "isothermal baths." The efficiency of the isothermal baths to maintain constant sample temperature is illustrated in Fig. 4, which compares the maximum temperature rise (ΔT_{max}) as a function of strain rate for samples initially at 20°C and tested in an isothermal ethanol bath and in air. In both air and ethanol, the sample temperatures increased with strain rate. The ΔT_{max} values were much higher for testing in air, reaching close to 90°C at the highest strain rate of 0.2 s^{-1}. In the ethanol bath, the effects of adiabatic heating could be reduced but not completely avoided. For example, with the strain rate of 0.2 s^{-1}, a temperature increase of about 50°C was recorded, while for the slowest strain rate of 0.002 s^{-1}, ΔT_{max} was about 5°C. Extrapolation of the data in Fig. 4 suggests that a strain rate of less than 0.001 s^{-1} would be required in order to develop near-isothermal conditions.

The important effects of adiabatic heating on the tensile deformation behavior of the 10MnAl steel are illustrated in Figs. 5 and 6. Figure 5 compares the engineering stress–strain behavior of samples tested at engineering strain rate of 0.002 s^{-1} in air and in an isothermal ethanol bath, both initially at 20°C. Both samples exhibit identical deformation behavior at low strains but diverge with an increase in strain, resulting in lower work-hardening rates and a lower (by about 50 MPa) UTS in the sample tested in air. As shown in Fig. 4, the maximum temperature rises due to adiabatic heating during the tests in air and ethanol were about 15°C and 5°C, respectively. Thus, the effective temperature of the specimen tested in air at the end of the test was approximately 10°C greater than for the specimen tested in ethanol. As a consequence of the higher temperature developed in the specimen tested in air, the austenite was more stable, leading to less deformation-induced martensite formation, and thus lower strain hardening and strength in comparison with the sample tested in ethanol. It is anticipated that, if a sample were to be tested in

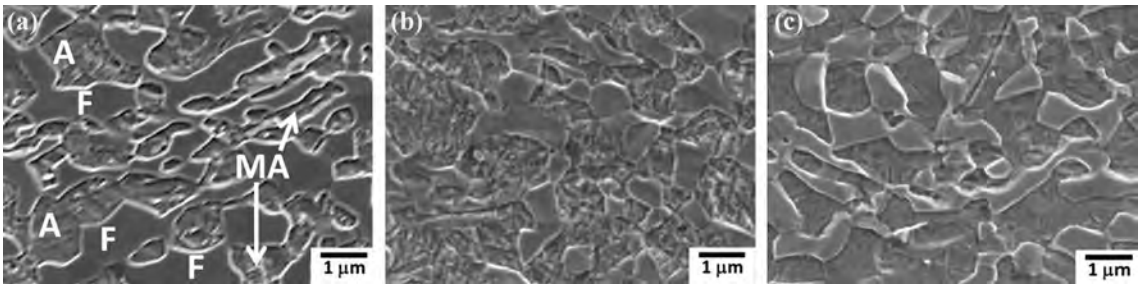

Fig. 3. Representative scanning electron micrographs of 10MnAl steel selected to show changes under deformation in isothermal baths. (a) As-annealed (undeformed), and deformed at 0.2 s^{-1} to a strain of 0.2 at (b) − 60°C and (c) 100°C (etched in 2% nital). Reprinted with permission from Ref. 3.

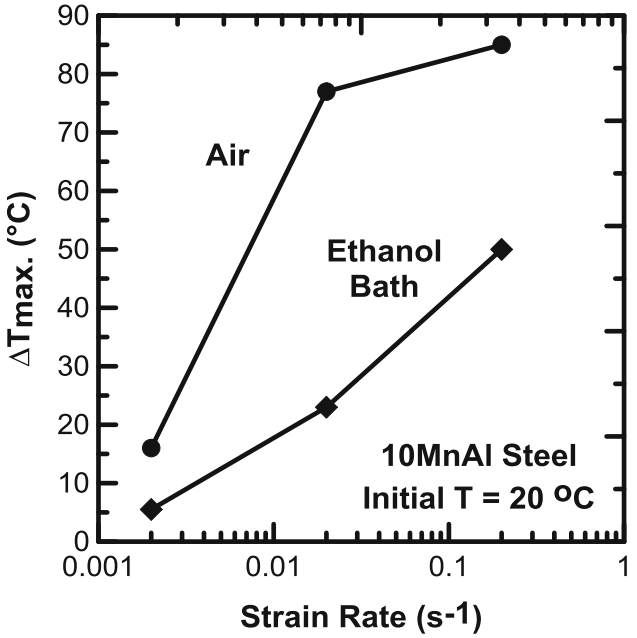

Fig. 4. Comparison of maximum increase in sample temperature from an initial temperature as function of imposed strain rate for samples tested in air and isothermal ethanol bath; both with an initial temperature of 20°C.

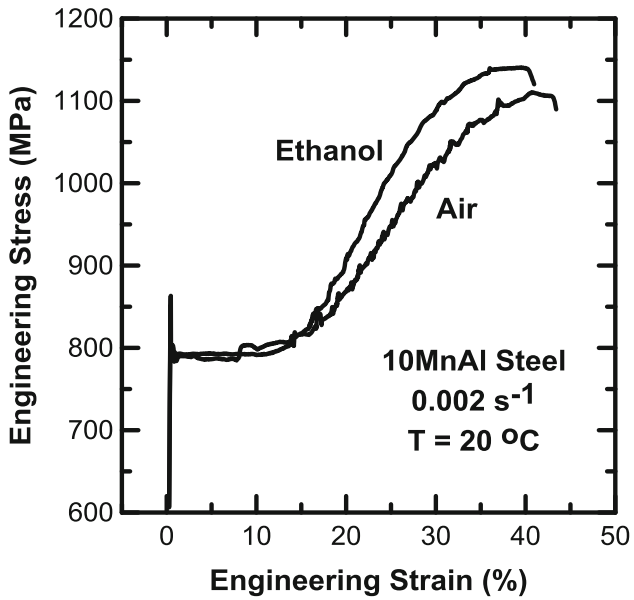

Fig. 5. Comparison of effects of environment on engineering stress–strain curves for samples of 10MnAl steel tested at an initial temperature of 20°C at 0.002 s^{-1}.

near-isothermal conditions, i.e., at strain rate of 0.001 s^{-1} or lower in ethanol as suggested by the data from Fig. 4, the resulting stress–strain curve would coincide with the data in ethanol in Fig. 5 at low strains but would plot at slightly higher stress values at high strains.

The effects of strain rate on deformation heating and stress–strain behavior are illustrated in Fig. 6 for samples tested in isothermal ethanol baths at engineering strain rates of 0.002 s^{-1} and 0.2 s^{-1}. Data are shown for samples initially at − 60°C (Fig. 6a), − 20°C (Fig. 6b), and 20°C (Fig. 6c). Also included in each figure are the maximum temperature increases measured just prior to fracture. For all three initial test temperatures, the tensile test at the higher strain rate (0.2 s^{-1}) exhibited less work hardening, lower UTS values, and significantly more adiabatic heating, leading to greater temperature increases than observed for the corresponding samples tested at the lower strain rate (0.002 s^{-1}).

At the higher strain rate, the yield plateau was higher at each test temperature than the yield plateau at the lower strain rate, leading to positive strain rate sensitivity of the 10MnAl steel. However, the behavior changed completely in the plastic deformation regions of the tensile curves. The specimens tested at the slower rate reached a higher UTS, demonstrating an apparent negative strain rate sensitivity of the steel. Consistent with the interpretation of the data in Fig. 5, it is concluded that the higher extent of adiabatic heating in the high strain rate tests increased austenite stability, leading to lower contributions of deformation-induced martensite to the overall strain-hardening behavior and strength.

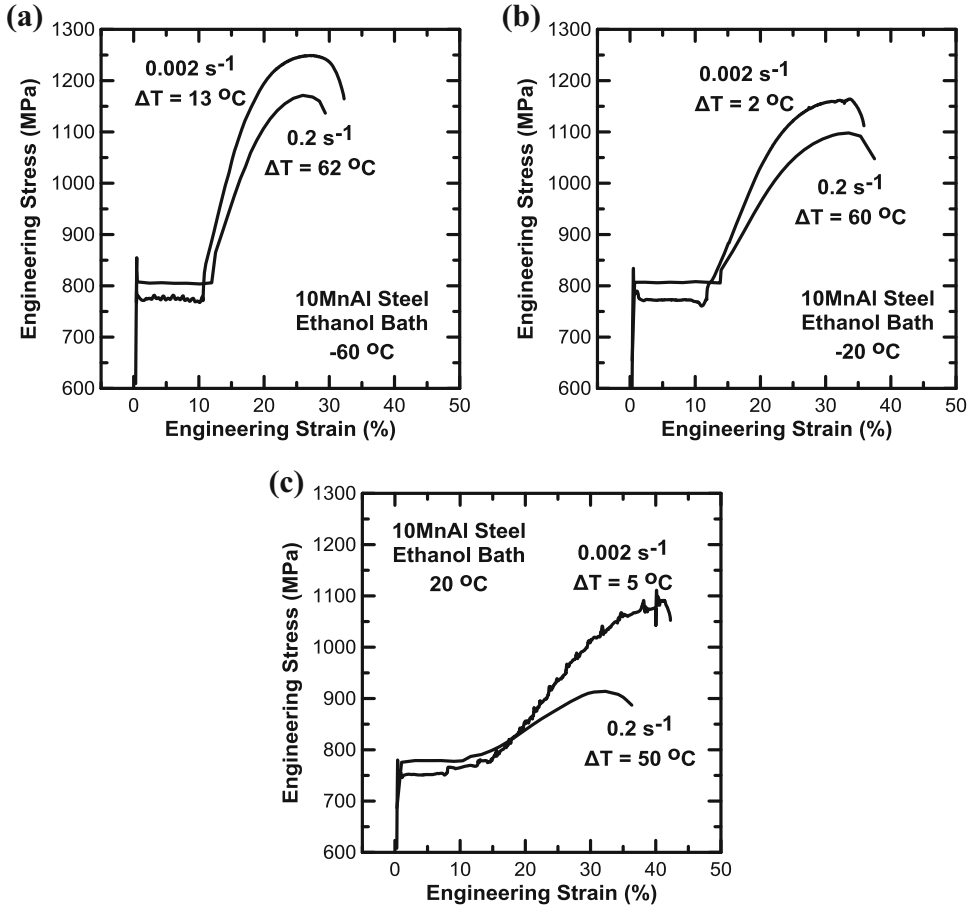

Fig. 6. Comparisons of effects of strain rate for tests at 0.2 s^{-1} and 0.002 s^{-1} on engineering stress–strain behavior of samples tested in isothermal ethanol baths at (a) − 60°C, (b) − 20°C, and (c) 20°C. The maximum temperature increase measured at the end of each test is also indicated by the respective ΔT values.

The results of this study highlight the importance of temperature on the deformation behavior of 10MnAl steel, and in particular the effects of temperature changes during deformation on the stress–strain behavior of the steel. As summarized by Pereira and Rolfe,[18] the phenomena of deformation-induced heating and frictional heating are well known and have been considered in multiple earlier publications, although limited attempts have been made to systematically experimentally validate predicted temperatures based on numerical models. In their study, Pereira and Rolfe modeled both friction and deformation heating and validated predictions based on measurements on a specialized laboratory forming press. One important outcome of their work was the prediction of die and blank temperatures for different steel grades, including AHSS.[18] The results of some of their predictions are adapted in Fig. 7, which shows the relationship between material strength and the maximum temperatures developed in the die and sheet blank. Calculations based on four steel grades showed systematic increases in both die and blank temperatures with material strength. With an increase in strength, die contact forces increased, leading to higher frictional heating and, depending on ductility, to higher contributions of adiabatic heating. Also included in Fig. 7 are approximate extrapolations for both the die and blank temperatures to the strength range consistent with the current study on 10MnAl medium-manganese steel. The extrapolation for the blank suggests that, in single-step forming operations, blank temperatures on the order of 130°C might be observed.

All of the materials considered by Pereira and Rolfe[18] had primarily stable ferritic microstructures. Except for potential contributions of dynamic strain aging as blank temperatures approach 200°C,[24] it is anticipated that the combined effects of temperature, adiabatic heating, and strain rate would be much less pronounced than would be observed for the medium-manganese steel considered here. Incorporation of the flow behavior of medium-manganese steels into meaningful numerical analyses of forming operations will require material models that include the strain, strain rate, and temperature dependence of the microstructural constituents, particularly deformation-induced martensite.

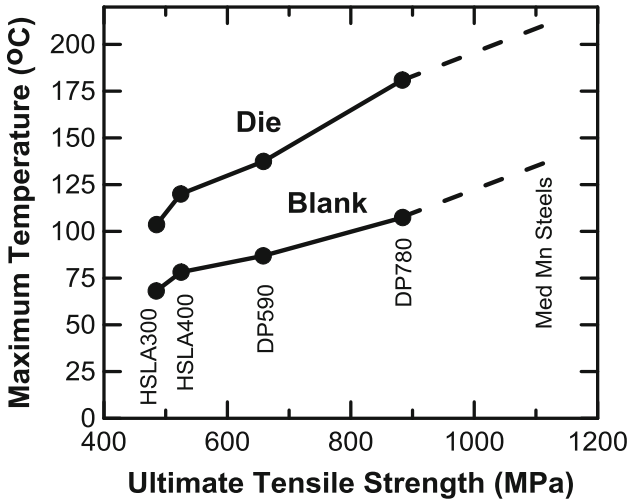

Fig. 7. Comparison of predicted die and blank temperatures during steady-state sheet metal forming for steels with different strengths based on properties of the indicated HSLA and DP steels. The dashed extrapolation was added to indicate potential temperature ranges for the medium-Mn steels considered in this paper. Adapted based on predictions of Pereira and Rolfe.[18]

The data presented in this paper suggest that predictions of the deformation behavior of medium-Mn steels would be complex, as the strain-hardening behavior depends sensitively on the deformation-induced transformation of retained austenite to martensite. Accurate numerical models of forming operations and material performance during crash situations must incorporate the effects of temperature and temperature changes during deformation on the microstructures and flow behavior of sheet steels in order to be able to predict meaningful forming loads and strain distributions in components. During forming and in a crash, heat generated by frictional forces and adiabatic heating is expected to contribute significantly to the response of medium-manganese steels and other new 3GAHSS grades with significant amounts of retained austenite, particularly at high processing rates consistent with automotive stamping operations.[25] Thus, predictions based only on quasistatic room-temperature tests are potentially misleading. Creation of truly isothermal test conditions may be of interest to obtain input data for models predicting material performance at a fixed temperature (be it during forming or crash), but this will be difficult to achieve. As a result, opportunities exist to systematically model and evaluate the effects of strain, strain rate, and temperature on martensite formation during deformation, verify model predictions based on experimental measurements, and incorporate these changes into new models to guide efficient production of automotive components from new austenite-containing 3GAHSS grades. As the importance of deformation-induced martensite formation is well known in austenitic stainless steels, it is further anticipated additional guidance for required modifications to model inputs may be found in forming analyses of stainless steels.

CONCLUSION

- The mechanical properties of a medium-Mn steel containing 10.1Mn-1.68Al-0.14C-0.2Si (wt.%) and high amount of retained austenite (57 vol.%) were shown to be sensitive to deformation conditions, namely strain rate and test temperature. The key parameter that influenced the mechanical properties of the 10MnAl steel was the stability of retained austenite during deformation.
- With increasing temperature in the range from − 60°C to 100°C, the austenite stability of the 10MnAl steel increased, leading to a decrease in tensile strength due to less transformation of retained austenite to martensite during deformation.
- During deformation, adiabatic heating, the extent of which increased with an increase in strain rate, contributed to stabilizing the austenite, leading to lower strain-hardening rates and strengths in comparison with testing conditions that minimized adiabatic heating. The temperature increase could be minimized by testing in isothermal liquid baths but was not eliminated over the strain rate range considered in this study.
- With increase in the imposed strain rate in the range of 0.002–0.2 s^{-1}, the 10MnAl steel exhibited negative strain rate sensitivity of flow stress due to the increase in austenite stability caused by adiabatic heating.
- During sheet metal deformation, as in forming and crash events, adiabatic heating and frictional forces can lead to significant temperature increases which alter the deformation behavior of medium-Mn sheet steels. The observations of this study suggest that material properties of medium-Mn steels used as inputs to forming models should incorporate changes in austenite stability during the forming process.

ACKNOWLEDGEMENT

The authors acknowledge support of the corporate sponsors of the Advanced Steel Processing and Products Research Center at the Colorado School of Mines. This material is based upon work supported by the Department of Energy National Energy Technology Laboratory under Award No. DE-EE0005976. This report was prepared as an account of work sponsored by an agency of the United States Government. Neither the United States Government nor any agency thereof, nor any of their employees, makes any warranty, express or implied, or assumes any legal liability or responsibility for

REFERENCES

1. P.J. Gibbs, E. De Moor, M.J. Merwin, B. Clausen, J.G. Speer, and D.K. Matlock, *Metall. Mater. Trans. A* 42A, 3691 (2011).
2. R. Rana, P.J. Gibbs, E. De Moor, J.G. Speer, and D.K. Matlock, *Steel Res. Int.* 86, 1139 (2015).
3. R. Rana, D.K. Matlock, J.G. Speer, and E. De Moor, in *Proceedings of the 1st International Conference on Automobile Steel and the 3rd International Conference on High Manganese Steels*, ed. By Haiwen Luo (Beijing, Metallurgical Industry Press, 2016) pp. 119–122.
4. D.W. Suh, J.H. Ryu, M.S. Joo, H.S. Yang, K.Y. Lee, and H.K.D.H. Bhadeshia, *Metall. Mater. Trans. A* 46A, 286 (2013).
5. Y. Ma, *Mater. Sci. Technol.* 33, 1713 (2017).
6. Y.-K. Lee and J. Han, *Mater. Sci. Technol.* 31, 843 (2015).
7. B.C. De Cooman, in *Automotive Steels: Design, Metallurgy, Processing and Applications*, ed. R. Rana and S. B. Singh (London: Elsevier, 2016), p. 317.
8. B. Hu, H. Luo, F. Yang, and H. Dong, *J. Mater. Sci. Technol.* (2017). https://doi.org/10.1016/j.jmst.2017.06.017.
9. D.K. Matlock and J.G. Speer, *Microstructure and Texture in Steels and Other Materials*, ed. by A. Haldar, S. Suwas, and D. Bhattacharjee (London: Springer, 2009) p. 185.
10. D.K. Matlock, J.G. Speer, E. De Moor, and P.J. Gibbs, *Eng. Sci. Technol. Int. J. (JESTECH)* 15, 1 (2012).
11. Y. Zhang, L. Wang, K.O. Findley, and J.G. Speer, *Metall. Mater. Trans. A* 48A, 2140 (2017).
12. G. Frommeyer, U. Brüx, and P. Neumann, *ISIJ Int.* 43, 438 (2003).
13. I. Tamura, *Metal. Sci.* 16, 245 (1982).
14. S. Curtze and V.-T. Kuokkala, *Acta Mater.* 58, 5129 (2010).
15. P. Hora, P. Peters, N. Manopulo, and M. Gorji, in *Proceedings of Advanced Constitutive Models in Sheet Metal Forming* (Zurich: Institute of Virtual Manufacturing, 2015), pp. 3–9.
16. S. Bruschi, T. Altan, D. Banabic, P.F. Bariani, A. Brosius, J. Cao, A. Ghiotti, M. Khraisheh, M. Merklein, and A.E. Tekkaya, *CIRP Ann. Manuf. Technol.* 63, 727 (2014).
17. M.A. Ablat and A. Qattawi, *Int. J. Adv. Manuf. Technol.* 89, 1235 (2017).
18. M.P. Pereira and B.F. Rolfe, *J. Mater. Process. Technol.* 214, 1749 (2014).
19. M. Callahan, O. Hubert, F. Hild, A. Perlade, and J.-H. Schmitt, *Mater. Sci. Eng. A* 704, 391 (2017).
20. Y.F. Shen, N. Jia, R.D.K. Misra, and L. Zuo, *Acta Mater.* 103, 229 (2016).
21. G.S. Langdon and G.K. Schleyer, *J. Strain Anal. Eng. Des.* 39, 71 (2004).
22. B.K. Choudhary, *Metall. Mater. Trans. A* 45A, 302 (2004).
23. G.B. Olson, in *Deformation, Processing, and Structure*, ed. by G. Krauss (Metals Park: ASM, 1984) pp. 391–424.
24. C.-C. Li and W.C. Leslie, *Metall. Trans. A* 9A, 1765 (1978).
25. P. Verleysen, J. Peirs, J. Van Slycken, K. Faes, and L. Duchene, *J. Mater. Process. Technol.* 211, 1457 (2011).